

22. LATE QUATERNARY TEXTURAL CHANGE OFFSHORE OF POINT CONCEPTION, SITE 1017, CENTRAL CALIFORNIA MARGIN¹

Richard J. Behl,² Ryuji Tada,³ and Tomohisa Irino⁴

ABSTRACT

Siliciclastic sedimentation at Ocean Drilling Program Site 1017 on the southern slope of the Santa Lucia Bank, central California margin, responded closely to oceanographic and climatic change over the past ~130 ka. Variation in mean grain-size and sediment sorting within the ~25-m-thick succession from Hole 1017E show Milankovitch-band to submillennial-scale variation. Mean grain size of the “sortable silt” fraction (10–63 μm) ranges from 17.6 to 33.9 μm (average 24.8 μm) and is inversely correlated with the degree of sorting. Much of the sediment has a bimodal or trimodal grain-size distribution that is composed of distinct fine silt, coarse silt to fine sand, and clay-size components. The position of the mode and the sorting of each component changes through the succession, but the primary variation is in the presence or abundance of the coarse silt fraction that controls the overall mean grain size and sorting of the sample. The occurrence of the best-sorted, finest grained sediment at high stands of sea level (Holocene, marine isotope Substages 5c and 5e) reflect the linkage between global climate and the sedimentary record at Site 1017 and suggest that the efficiency of off-shelf transport is a key control of sedimentation on the Santa Lucia Slope. It is not clear what proportion of the variation in grain size and sorting may also be caused by variations in bottom current strength and in situ hydrodynamic sorting.

INTRODUCTION

Ocean Drilling Program (ODP) Site 1017 is located on the southern slope of the Santa Lucia Bank in 955 m of water, ~50 km west of Point Conception and Point Arguello on the central Californian margin (Fig. 1; Lyle, Koizumi, Richter, et al., 1997). This location is of interest because of its setting beneath a persistent modern upwelling structure within the California Current system and by its location at the boundary between two oceanographic provinces of the eastern boundary current system—the southern California Bight and the Strait of Juan de Fuca to Point Conception segment (Brink et al., 1984; Hickey, 1998). The site is also particularly important because of its close proximity to Santa Barbara Basin where recent studies have found evidence for rapid millennial-scale climatic and oceanographic fluctuations during the late Quaternary that reflect oceanic changes in circulation and intermediate water ventilation (Kennett, Baldauf, and Lyle, 1995; Kennett and Ingram, 1995; Behl and Kennett, 1996; Cannariato et al., 1999).

Five holes were cored at this site with the last (Hole 1017E) dedicated to a high-resolution study of the late Quaternary paleoceanography of this region (see Tada et al., Chap. 25, this volume). The three cores from Hole 1017E (~25 m in aggregate length) were sliced into >850, 3-cm increments, each of which was split and distributed for determination of isotopic, elemental, organic geochemical, biomarker, magnetic, textural, and fabric characteristics of the sediments by various researchers. The study presented here focuses on the character and nature of textural change (grain size and sorting) at Site 1017 over the past ~130 ka and throughout the uppermost 25 m of sediment. This data provides insight into how the sedimentary record was physically influenced by changes in the strength of intermediate water-depth contour currents and eddies, by variation in the effectiveness of

offshore transport related to sea level, or by climatically related changes in river discharge.

METHODS

The sealed core sections from Hole 1017E were split in half lengthwise, described, and sampled at Texas A&M University approximately three months after the completion of ODP Leg 167. Curated depths (meters below seafloor [mbsf]) were corrected to account for gas expansion, cracks, and missing material at core breaks (see Kennett et al., Chap. 21, this volume; Tada et al., Chap. 25, this volume). Two textural data sets were generated from splits of the same samples comprising every 3 cm of Cores 167-1017E-1H, 2H, and 3H. Multiple methods of grain-size analysis are available to researchers. Each has its own advantages or drawbacks in what is actually measured (e.g., particle diameter, volume, settling rate, scattering effects, etc.), the accuracy and precision of analyses, size range analyzed in a single step or multiple iterations, and in the required volume of sample (Singer et al., 1988; McCave and Syvitski, 1991; McCave et al., 1995). The methods employed in our study were largely determined by the instruments available at our institutions; both are previously reviewed, standard methodologies (Singer et al., 1988; McCave and Syvitski, 1991). The first sample set (LB) was analyzed at California State University at Long Beach with a Coulter multisizer using the electrical sensing zone technique (which measures the displaced volume of individual particles). This data set includes nearly all of the 3-cm samples. The second set (TU) was analyzed at Tokyo University with a Horiba LA-920 grain size analyzer by laser diffraction (which measures the angular scattering of suspended particles). This data set is primarily restricted to the intervals 0–224 and 711–889 corrected centimeters below seafloor (cmbsf), in which every other 3-cm increment was analyzed. In both sample sets, sediments were disaggregated, rinsed of sea salt, cleaned of calcium carbonate (hydrochloric acid or acetic acid dissolution) and organic matter (hydrogen peroxide oxidation), and dispersed (sodium hexametaphosphate or sodium pyrophosphate). These steps are required to accurately measure the grain-size distribution of the siliciclastic fraction of the sediment with minimal complications from including materials with different densities, specific surface areas, or adhesive

¹Lyle, M., Koizumi, I., Richter, C., and Moore, T.C., Jr. (Eds.), 2000. *Proc. ODP, Sci. Results*, 167: College Station TX (Ocean Drilling Program).

²Department of Geological Sciences, California State University at Long Beach, 1250 Bellflower Blvd., Long Beach CA 90840, USA. behl@csulb.edu

³Geological Institute, University of Tokyo, 7-3-1 Hongo, Tokyo 113, Japan.

⁴Department of Earth and Planetary Sciences, Hokkaido University, Kita-10, Nishi-8, Kitaku, Sapporo, 060-0810, Japan.

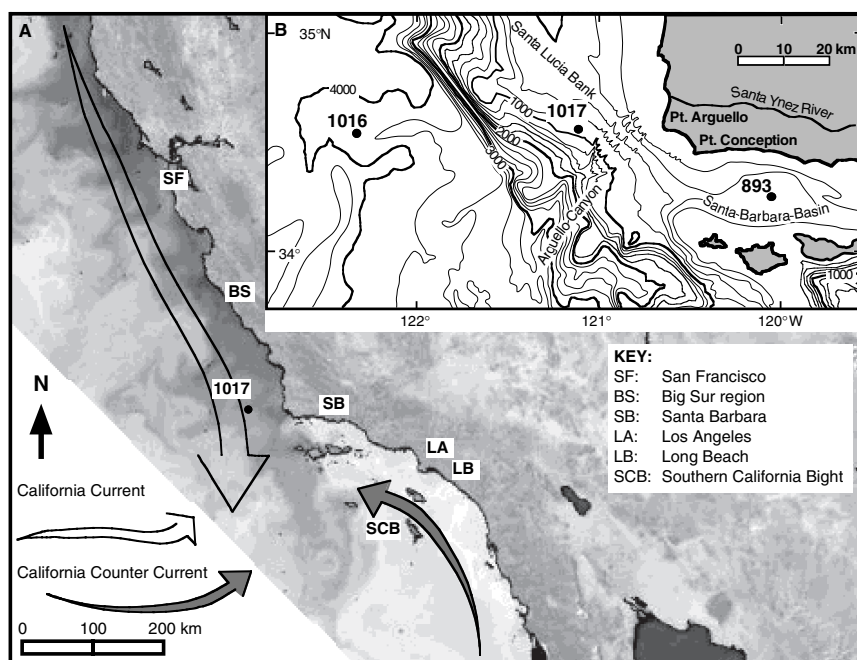


Figure 1. Location map. **A.** Annotated coastal zone color scanner image of currents along the California margin showing the location of Site 1017 and geographical reference points. **B.** Inset map showing ODP Sites 1016, 1017, and 893; bathymetry of region; and locations of the Santa Ynez River, Santa Lucia Bank, Arguello Submarine Canyon and feeder canyons, and Santa Barbara Basin.

properties. Set LB was sieved to remove any sand-sized particles ($>63\ \mu\text{m}$) before analysis. Set TU was initially treated with a buffered dithionite-citrate solution to remove Fe-Mn oxides (Tada et al., Chap. 25, this volume). Both sample sets retained small amounts of opaline biosiliceous debris (generally $<5\%$).

Statistical analysis of the grain-size distribution data provided median, mode, and mean grain sizes and sorting indicators (e.g., standard deviation) for each sample. These statistics can be derived for the entire measured spectrum ($2\text{--}63\ \mu\text{m}$ for set LB, $0.02\text{--}2000\ \mu\text{m}$ for set TU) or only from some selected subset of that spectrum. We adopt the procedure of McCave et al. (1995) to present statistics from the 10- to $63\text{-}\mu\text{m}$ -size range (the “sortable silt” fraction) in addition to those of the entire measured range. This restricted size range forms the noncohesive fraction of silt; therefore, changes in the mean size and sorting of this sediment are most likely to reflect response to hydrodynamic processes (McCave et al., 1995). Because many sediment samples analyzed display a bimodal grain-size distribution, selected samples were deconvolved by an iterative curve-fitting method to resolve the modes, sorting, and relative proportions of the separate size components that make up the entire distribution. These size components are correlated with chemical and mineralogical components via factor analysis (Tada et al., Chap. 25, this volume; Irino and Pederesen, Chap. 23, this volume).

Data are plotted with depth (cmbsf) and also with age based on the radiocarbon and oxygen isotope age model of Kennett et al. (Chap. 21, this volume) from 0 to 58.956 ka ($0\text{--}1224.2$ cmbsf). This paper also uses a linear extension of this model to 129.84 ka (2487.3 cmbsf), based on correlation between shipboard measurements of color reflectance (compositional proxy) and U_{37}^k values (near surface temperature proxy; Lyle, Koizumi, Richter, et al., 1997) with the standard marine oxygen isotope record, placing the bottom of the hole at approximately the middle of Termination 2 (marine isotope Stage [MIS] datum 6.0; Martinson et al., 1987).

RESULTS

Sedimentologic Overview

The late Quaternary succession at Site 1017 consists primarily of siliciclastic silty clay to clayey silt, with minor amounts of biogenic

calcium carbonate ($<10\%$; foraminifers and nannofossils), and rare biogenic opal ($\sim 2\%$; chiefly fragments of sponge spicules, with fewer diatoms; Lyle, Koizumi, Richter, et al., 1997; Tada et al., Chap. 25, this volume). Rare, centimeter-scale, bioclastic or siliciclastic sand layers are concentrated between two intervals, 320–500 and 1390–1470 cmbsf, representing MISs 2 and 4, respectively—both sea-level lowstands. Sand layers are typically sharp based and some are normally graded. Sands are primarily quartzofeldspathic and contain variable, generally minor, quantities of mica and abraded bioclasts. Trace amounts of amphibole, augite, and a green garnet (possibly uvarovite) are present in most sands and coarse silt fractions.

With the exception of sand layers and sparse, millimeter-scale, silty laminations discernible by X-rays, the upper Quaternary sequence is bioturbated and massive. Near-continuous burrowing is displayed by computed tomographic (CT) vertical X-rays of sediment slabs and CT-scans of bedding parallel slices (Behl et al., 1997; Morris and Behl, 1998; Fig. 2). *Chondrites* and *Planolites* trace fossils are present, but most common are unidentified millimeter- to centimeter-diameter vertical to nearly horizontal burrows in addition to pervasive mottling. Ongoing bioturbation (up to tens of centimeters deep) likely obliterated all but the most rapidly deposited and buried sedimentary structures.

Set LB

The mean grain size for the entire measured spectrum ranges from 7.4 to $30.3\ \mu\text{m}$ though the succession, with an average value of $19.5\ \mu\text{m}$ (Table 1; Fig. 3). The mean of the sortable silt fraction ($10\text{--}63\ \mu\text{m}$) ranges from 17.6 to $33.9\ \mu\text{m}$ (average $24.8\ \mu\text{m}$). The degree of sample-to-sample variation is fairly high, regularly fluctuating $2\text{--}4\ \mu\text{m}$ between adjacent samples, yet certain trends and cyclicities can be discerned in the succession, especially within a smoothed record (21-pt. running average; i.e., 63 cm or ~ 3 k.y.). The uppermost 2200 cm (0 to ~ 113 ka) is distinctly coarser ($20.0\ \mu\text{m}$ average whole spectrum; $25.2\ \mu\text{m}$ average sortable silt) than the lowermost 400 cm ($\sim 113\text{--}130$ ka, $16.1\ \mu\text{m}$ average whole spectrum, and $21.8\ \mu\text{m}$ average sortable silt). The upper section consists of ~ 12 irregular coarse to fine cycles (smoothed record) with the lower interval spanning another two. Cycles range from ~ 120 to ~ 250 cm in thickness with an average period of ~ 8.5 k.y. in the upper section and 11.2 k.y. in the

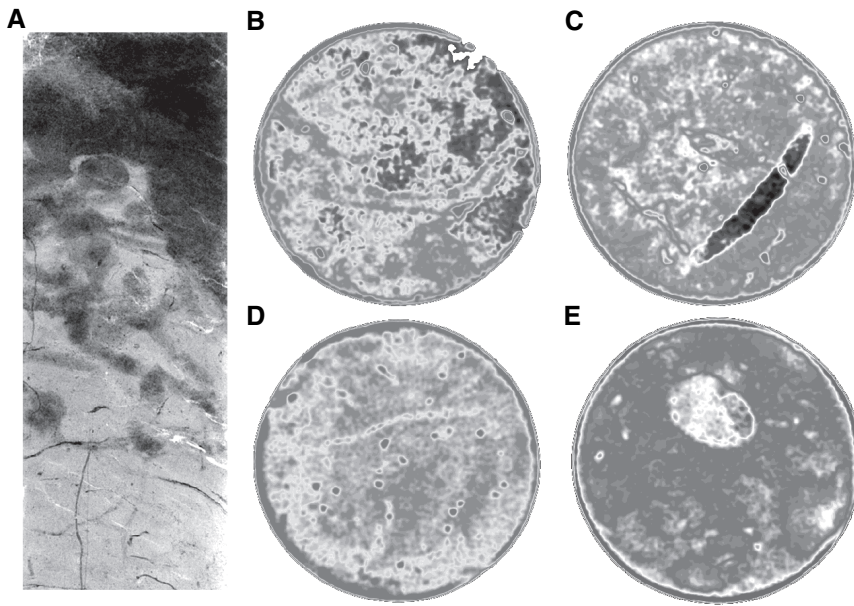


Figure 2. X-ray and CT-scans showing heavily bioturbated fabric of sediment at Site 1017. **A.** X-ray of Sample 167-1017E-2H-7, 60–68 cm (1465–1473 cmbsf) showing bioturbated contact between turbidite sand layer and underlying silty clay. Thin black stringers are pyritized burrows. **B–E.** Bedding-parallel CT scans showing variation in scale and orientation of burrows. **B.** Sample 167-1017E-2H-4, 65 cm (1059 cmbsf). **C.** Sample 167-1017E-2H-4, 125 cm (1114 cmbsf). **D.** Sample 167-1017E-2H-6, 5 cm (1278 cmbsf). **E.** Sample 167-1017E-2H-6, 75 cm (1342 cmbsf).

Table 1. Grain-size data from set LB and oxygen isotope data.

Hole, core, section	Interval (cm)	Depth (cmbsf)	Depth (mbsf)	Corrected depth (cmbsf)	Age (ka)	Grain-size data			21-pt. SS			$\delta^{18}\text{O}$ bulloides	$\delta^{13}\text{C}$ bulloides	Site 893 isotope age	Site 893 benthic O-iso PDB		
						Mean	Median	SD	Mean	SD	SS mean					SS median	SS SD
1017E-																	
1H-1	0-3	1.5	0.015	1.4	0.064	14.55	12.91	8.496			18.73	16.92	7.72			0.051	2.413
1H-1	3-6	4.5	0.045	4.3	0.197	13.99	12.44	8.913			19.58	18.27	7.22			0.280	2.577
1H-1	6-9	7.5	0.075	7.2	0.330	18.56	16.13	11.750			23.41	21.14	10.30				
1H-1	9-12	10.5	0.105	10.1	0.463	18.75	16.78	11.230			22.77	20.56	10.00			0.556	2.348
1H-1	12-15	13.5	0.135	12.9	0.591	19.71	18.09	11.090			23.39	21.72	9.74			0.828	2.333
1H-1	15-18	16.5	0.165	15.8	0.724	27.99	27.24	13.240			29.89	28.84	12.20			0.828	
1H-1	18-21	19.5	0.195	18.7	0.857	27.50	26.73	13.980			30.26	29.27	12.40			1.117	2.391
1H-1	21-24	22.5	0.225	21.6	0.989	28.08	27.89	13.790			30.72	30.04	12.20			1.410	2.337
1H-1	24-27	25.5	0.255	24.4	1.118	22.56	20.60	13.240			26.45	24.23	11.70			1.713	2.306
1H-1	27-30	28.5	0.285	27.3	1.251	18.38	16.66	10.660			22.53	20.82	9.14			2.012	2.196

Notes: SD = standard deviation, PDB = oxygen and carbon isotopes with respect to PDB standard, SS = sortable silt. Oxygen isotope data from Kennett (1995) and Kennett et al. (Chap. 21, this volume).

This is a sample of the table that appears on the volume CD-ROM.

lower part (Fig. 4). Stratification is poorly developed, and the cycles expressed by variation in mean grain size and sorting are not visually distinct or sharply bounded.

The degree of sediment sorting (as shown by the standard deviation of the grain-size distribution) is inversely related to grain size (Figs. 3, 4). Each coarser interval is associated with a corresponding increase in the standard deviation of the grain size. The sediment is best sorted near the top and bottom of the succession at ~0–220, 1900–1990, and 2160–2487 cmbsf (0–10 ka/Holocene, 97–102 ka/MIS 5c, and 111–130 ka/MIS 5e, respectively; Figs. 3, 4).

Set TU

Grain-size distributions of samples were analyzed to resolve the relative contributions and modes of different grain-size components. In particular, we focused on two intervals in the Holocene and MIS 3, including every other 3-cm increment (6-cm spacing). Most samples are unimodal or bimodal and have fine tails, allowing us to resolve the spectrum into two or three components with individual log normal distributions (Fig. 5; see Tada et al., Chap. 25, this volume, for details). The principal mode is located between 8 and 15 μm (i.e., chiefly fine silt); lesser components have modes between 2 and 4 μm (i.e., clay) and 39 and 73 μm (coarse silt to very fine sand; Table 2).

The fine silt component makes up 59%–86% of the samples by volume; clay, 5%–27%; and coarse silt, 0%–28%. The modes and contribution of each of these components varies within the stated ranges. The greatest variation is in the abundance of the coarse silt to fine sand fraction, which covaries with the mean grain size (Set LB; Figs. 6, 7). This relationship suggests that the principal control of textural variation at Site 1017 is the presence or absence of the coarse silt fraction.

Superimposed on the larger scale trends and meter-scale cycles are decimeter-scale oscillations in mean grain size, standard deviation, and the contribution of the coarse silt fraction. These cycles and the negative correlation between grain size and “sorting” are well illustrated in two expanded profiles through the Holocene and part of MIS 3 (Figs. 6, 7). Recognition of the bimodal or trimodal grain-size distribution demonstrates that a larger standard deviation does not reflect the degree of sediment sorting but, instead, the relative abundance of the three grain-size components.

DISCUSSION

Orbital, suborbital, and higher frequency (millennial) variation is clearly exhibited by fluctuations in mean grain size, sorting, and pro-

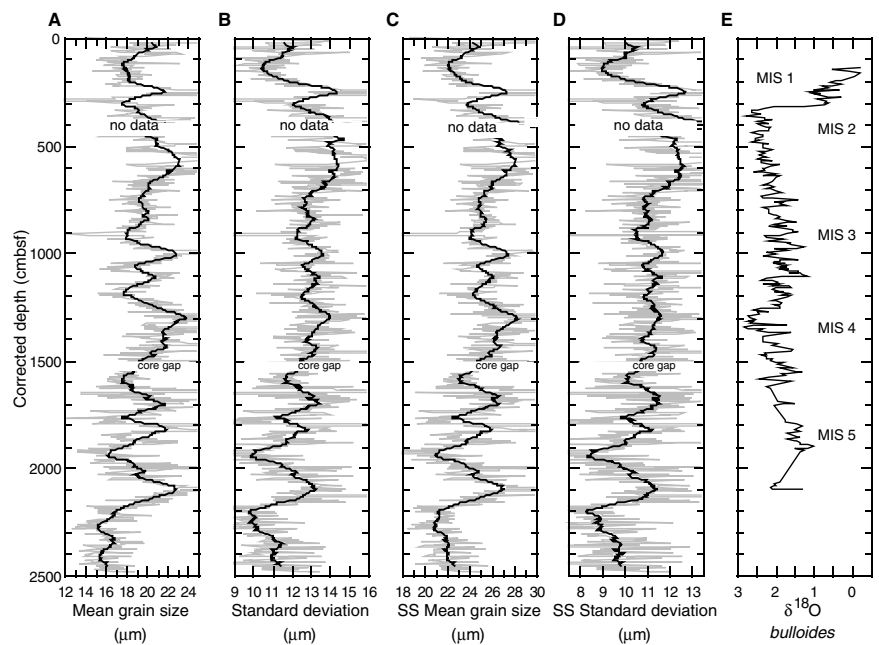


Figure 3. Mean grain size and standard deviation with 21-pt. running averages for Hole 1017E vs. depth. **A, B.** Entire measured spectrum. **C, D.** Sortable silt (SS) (10–63 μm). **E.** Oxygen isotopes of planktonic foraminifers (Kennett et al., Chap. 21, this volume).

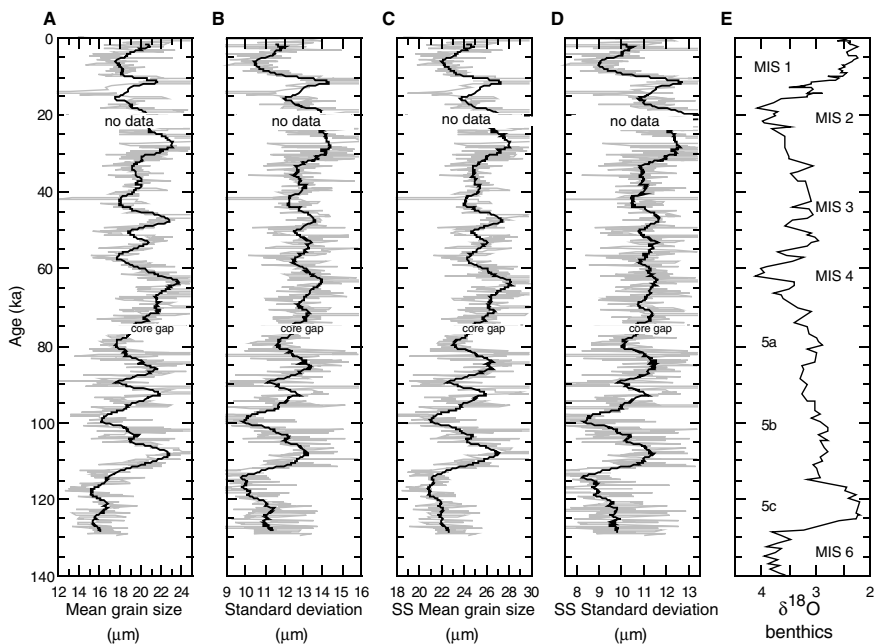


Figure 4. Mean grain size and standard deviation with 21-pt. running averages for Hole 1017E vs. age. **A, B.** Entire measured spectrum. **C, D.** Sortable silt (SS) (10–63 μm). **E.** Benthic oxygen isotopes from nearby Site 893 (Kennett, 1995).

portions of the grain-size fractions. An ~10,000-yr cyclicality is most strongly shown throughout the succession by changes in grain-size sorting. In general, grain size decreases and sorting increases (standard deviation decreases) during warmer intervals (low $\delta^{18}\text{O}$ of planktonic foraminifers) with higher sea level. Clearly, sedimentation at Site 1017 was strongly influenced by climatic and oceanographic oscillation, yet the exact mechanisms are not easily resolved. Below, we discuss some of the oceanographic and bathymetric constraints and lines of evidence important to consider in the interpretation of the late Quaternary record.

The slope setting (955 m) of Site 1017 is bounded upslope to the north by the Santa Lucia Bank and to the northeast by the continental shelf, and downslope to the south by the Arguello Submarine Canyon and to the east and southeast by a series of upper slope feeder canyons (Fig. 1). Siliciclastic sediments, which dominate this setting (Lyle, Koizumi, Richter, et al., 1997; Tada et al., Chap. 25, this volume), are

derived from riverine sources in the Santa Ynez, Santa Maria, and Big Sur regions of the California coast (Iriño and Pedersen, Chap. 23, this volume). Neritic sediment transport in the coastal zone and outer shelf is to the south under the influence of littoral drift and the equatorward-flowing California Current, respectively. Frequent, volumetrically minor, graded sand layers at Site 1017 indicate that some turbidity currents flowed directly down the slope or spilled out of the Arguello Submarine Canyon and its feeder system to flow over the southern Santa Lucia Slope. These coarse-grained turbidites are concentrated within two intervals between 320 and 510 cmbsf and 1390 and 1470 cmbsf, which were deposited during the MISs 2 and 4 lowstands. The ultimate source of the coarsest sediments is the nearshore region to the north and northeast (Big Sur and Santa Maria areas; Trask, 1952) where sands of similar composition can be found (including beach lag deposits nearly identical to a remarkable heavy mineral-, zircon-, and spinel-enriched sand layer present at 507

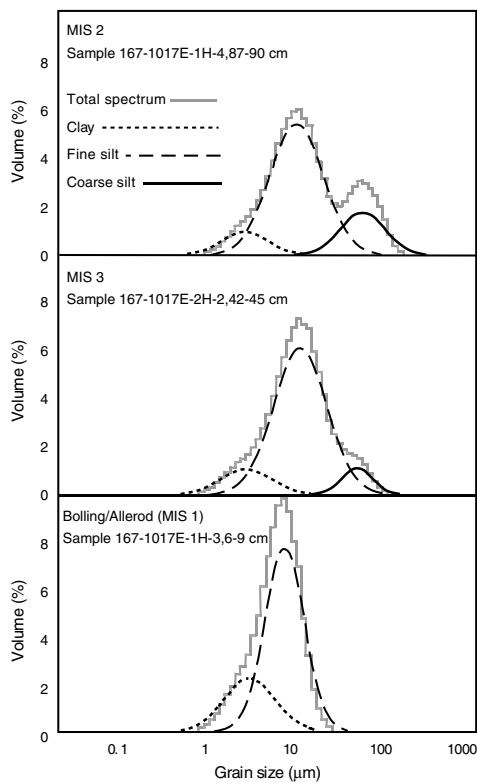


Figure 5. Examples of bimodal grain-size distribution resolved into two or three components with log normal distributions. The abundance and position of the modes of each component vary through the stratigraphic succession.

cmbsf in Hole 1017E). The elemental composition of even the finest silt and clay fraction of the sediment deposited during MISs 2 and 4 lowstands has a distinctly mafic provenance, most likely from the Mesozoic Franciscan Complex that outcrops along the central California coast north of Site 1017 (Iriño and Pedersen, Chap. 23, this volume). Longshore transport of sand from the north was increasingly diverted into the feeder canyons adjacent to Site 1017 (Fig. 1) during intervals of lower sea level and prevented from continuing on into the Santa Barbara Basin to the east (Behl, 1995) as it does during the present highstand.

In addition to the southward (equatorward) flow and transport due to the California Current (0–500 m depth) and shallow littoral currents, the margin is also influenced by the poleward-flowing California Undercurrent (Hickey, 1979). In modern studies, this current is strongest at 150–300 m water depths with peak speeds ~30–50 cm/s. During winters and other periods of low equatorward wind stress, the countercurrent's flow can extend all the way to the seafloor (~1000 m), albeit at lower velocities (Ramp et al., 1997). A deeper (~300–500 m) and weaker, seasonal equatorward undercurrent also flows over the continental slope as part of the California Current system (Hickey, 1998). At present, the highest velocity flows in both undercurrents are considerably shallower than the seafloor at Site 1017 (955 m), but it is possible that these oceanic currents may have influenced sediment transport and sorting at Site 1017 in the past. This could have occurred either directly, by expansion or deepening of the undercurrents to the seafloor at 1000 m, or indirectly, by resuspending and transporting sediment initially deposited upslope from this site. Both undercurrents can be disrupted and even reversed by large cyclonic and anticyclonic eddies offshore of northern and central California that may reach the seafloor in water as deep as 2000 m (S.R. Ramp, pers. comm., 1998).

Textural variation in the stratigraphic succession at Site 1017 was possibly influenced by either (1) the effects of sea-level fluctuation on offshore transport in the manner postulated and documented by sequence stratigraphers (e.g., Wilgus et al., 1988; Van Wagoner et al., 1990), (2) by fluctuation in the strength of bottom currents passing over the continental slope (Hollister and Heezen, 1972), or (3) by both. If grain size on the Santa Lucia Slope was primarily controlled by current action (i.e., coarser intervals are contourites), then both mean grain size and sediment sorting should be positively correlated (McCave, 1985). As current strength increases, so should grain size and sorting as the finer fraction of the noncohesive “sortable silt” is resuspended and removed, leaving behind a narrower spectrum of coarser silt and/or fine sand (McCave et al., 1995). This is not the case for the upper Quaternary succession at Site 1017, where grain size is negatively correlated with sorting, in which larger mean diameter is almost always associated with a greater standard deviation (poorer sorting). This relationship is explained by inspection of the relative contributions and modes of the two or three distinct components resolved from deconvolution of the grain-size distributions (data set TU). These grain-size spectra show that samples with coarser mean grain sizes are more poorly sorted, chiefly because of the presence of the coarse silt component (Fig. 5).

If sea level was the primary control of textural variation at Site 1017, then increased grain size may reflect enhanced resuspension and transportation off a narrowed and shallower shelf during times of lowered sea level (i.e., MIS 3 stadials and MISs 2, 4, and 6). Increased quantities of sediment could have been transported more or less directly downslope by nepheloid plumes and turbidity currents with some deflection by contour-following undercurrents. An alternate possibility is that off-shelf sediment transport was primarily routed through the feeder canyons to the east and southeast into the Arguello Submarine Canyon (Fig. 1). Hyperpycnal flow (possibly fed by suspended sediments from the Santa Ynez River) or low-density turbidites could easily ride up the right bank of the canyons (Mulder and Syvitski, 1995; Normark et al., 1998) and blanket the southern Santa Lucia Slope with fine-grained deposits. In both sea-level related scenarios, grain size and sorting on the slope would be modified primarily by the addition of the coarser silt fraction from shelfal regions to the finer hemipelagic sediments of the upper slope. Either mechanism could produce the thin intervals of faint silty laminations or sand layers that are intermittently present in this stratigraphic sequence (Tada et al., Chap. 25, this volume). The importance of sea level is also indicated by the observation that the finest mean grain size and best sorting (lowest standard deviation) corresponds to the highest sea level of this interval ~130–120 ka (Neumann and Hearty, 1996). Elemental geochemistry by Iriño and Pedersen (Chap. 23, this volume) indicates increased contribution of mafic and ultramafic components to the sediment during the last glacial maximum compared with MIS 1 (Holocene). We, too, find trace amounts of augite and uvarovite (a Cr-rich garnet)—two minerals associated with mafic and metamorphic (serpentinite) components of the Franciscan Formation that outcrops in the central Californian Big Sur region (Trask, 1952; Fig. 1)—consistently present in the coarse and fine silt fractions of samples taken from coarser intervals, but only rarely present in the coarse silt fractions of samples from finer intervals and never in their fine silt fraction. These data support the hypothesis that the coarser sediments represent increased downslope transport from the central Californian coast.

It is possible that individual grain-size components, especially the fine and coarse silt fractions, are not derived from different sources (i.e., shelf turbidites vs. hemipelagic sediment) but may represent episodic differences in the strength of bottom currents. Because each sample spans ~150-yr accumulation, the grain-size spectra may integrate sediments deposited under entirely different flow conditions. In this scenario, the coarse silt component would represent deposition during higher than average current flow rates. Although variability in

Table 2. Grain-size data from set TU presented as modes and percentages of the three resolved fractions.

Depth (mbsf)	Corrected depth (cmbsf)	Age (ka)	Fine mode	Medium mode	Coarse mode	Percentage fine	Percentage medium	Percentage coarse
10.5	10.1	0.5	3.2	12.7	60.3	12.2	65.9	21.9
16.5	15.8	0.7	3.3	14.9	58.2	10.0	71.0	19.0
22.5	21.6	1.0	2.9	13.3	59.7	9.9	68.6	21.5
28.5	27.3	1.3	2.9	12.7	58.4	10.5	71.1	18.4
34.5	33.0	1.5	3.0	13.2	60.0	11.1	68.2	20.7
40.5	38.8	1.8	3.4	13.6	57.1	12.8	64.5	22.7
46.5	44.5	2.0	3.0	12.7	59.4	11.4	69.6	19.0
52.5	50.3	2.3	3.0	13.1	56.6	10.8	70.4	18.8
58.5	56.0	2.6	3.0	12.9	57.1	11.2	73.1	15.7
64.5	61.8	2.8	3.6	13.3	57.0	13.8	64.6	21.6

This is a sample of the table that appears on the volume CD-ROM.

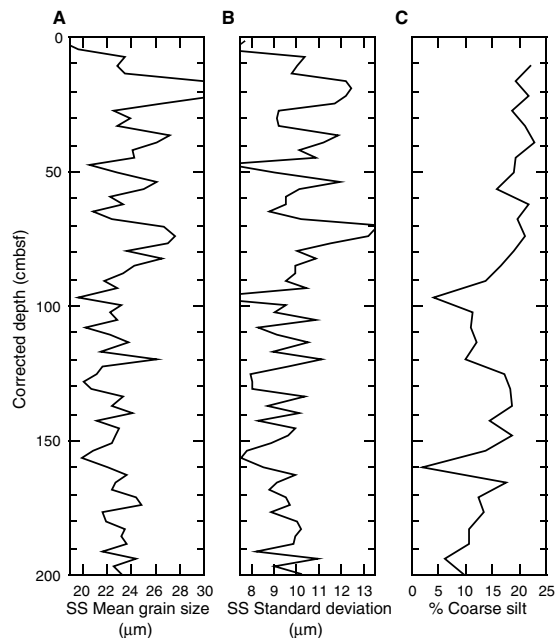


Figure 6. Expanded presentation of Holocene (MIS 1) succession, 0–200 cmbsf (~0–9 ka). **A.** Mean grain size of sortable silt (SS) (10–63 μm). **B.** Standard deviation of sortable silt (10–63 μm). **C.** Percentage coarse silt to fine sand component of set TU.

the location, persistence, and size of mesoscale eddies along the California margin may have produced significant variations in deep geostrophic flow (e.g., the “benthic storms” of Hollister and McCave, 1984), we do not know why contour current flow would be so distinctly bimodal as to produce separate grain-size classes instead of varying continuously over a range of velocities.

CONCLUSIONS

Siliciclastic sedimentation at Site 1017 on the southern slope of the Santa Lucia Bank, central California margin, responded closely to paleoceanographic and paleoclimatic change over the past ~130 ka. The ~25-m-thick succession from Hole 1017E displays Milankovitch-band to submillennial-scale variation in mean grain size and sediment sorting. Cycles with ~10,000-yr periodicity are the most prominent alternations in the record. Mean grain size of the “sortable silt” fraction (10–63 μm) ranges from 17.6 to 33.9 μm (average 24.8 μm). Much of the sediment is bimodal or trimodal and composed of fine silt (mode between 8 and 15 μm), coarse silt to fine sand (mode between 39 and 73 μm), and clay (mode between 2 and 4 μm) compo-

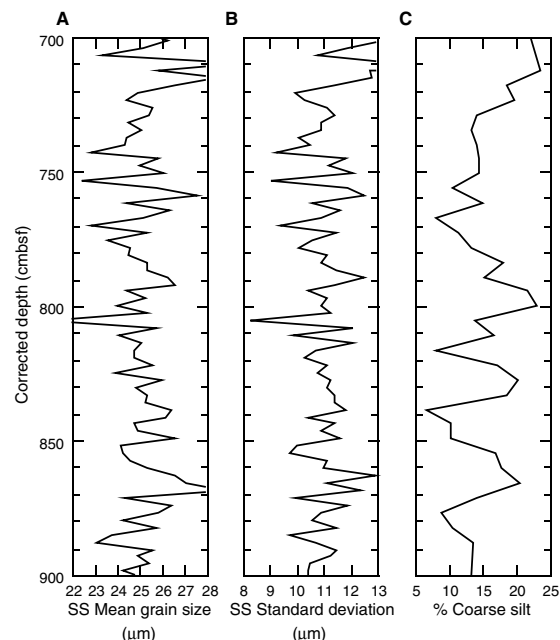


Figure 7. Expanded presentation of part of MIS 3 succession, 700–900 cmbsf (~31–41 ka). **A.** Mean grain size of sortable silt (SS) (10–63 μm). **B.** Standard deviation of sortable silt (10–63 μm). **C.** Percentage coarse silt to fine sand component of set TU.

nents. The position of the mode and the sorting of each component changes through the succession, but the primary variation is in the presence or abundance of the coarse silt fraction. This component is the key variable controlling the overall mean grain size and sorting of the entire sample. The occurrence of the best-sorted, finest grained sediment at highstands of sea level (Holocene; MISs 5c and 5e) reflects the linkage between global climate and the sedimentary record at Site 1017. Coarser sediments with geochemical and mineralogical indications of a Franciscan provenance are associated with sea-level lowstands. It is still unclear how much of the overall variation in grain size and sorting is caused by changes in the relative contribution of shelfal export vs. hemipelagic sedimentation or by variations in bottom current strength and in situ hydrodynamic sorting.

ACKNOWLEDGMENTS

This paper was greatly improved by the critical reviews of Adrian Cramp, Peir Pufahl, Wonn Soh, and the ODP editors. We thank Geraldine Aron, Raffie Barsamian, Barry Dalkey, Samuel deHaas, and Darrin Arthur for their assistance in performing nearly 1000 grain-

size measurements. This research was supported by a JOI/U.S. Science Support Program grant and a Grant-in-Aid for Scientific Research of the Ministry of Education, Science, and Culture of Japan (No. 08458141).

REFERENCES

- Behl, R.J., 1995. Sedimentary facies and sedimentology of the late Quaternary Santa Barbara Basin, Site 893. In Kennett, J.P., Baldauf, J.G., and Lyle, M. (Eds.), *Proc. ODP, Sci. Results*, 146 (Pt. 2): College Station, TX (Ocean Drilling Program), 295–308.
- Behl, R.J., and Kennett, J.P., 1996. Brief interstadial events in the Santa Barbara Basin, NE Pacific, during the last 60 kyr. *Nature*, 376:243–246.
- Behl, R.J., Morris, R.M., and Kennett, J.P., 1997. Late Quaternary paleoxygenation of the Central California Margin, ODP Site 1017, as shown by CT-scans. *Eos*, 78:F369.
- Brink, K.H., Stuart, D.W., and Van Leer, J.C., 1984. Observations of the coastal upwelling region near 34° 30'N off California: spring 1981. *J. Phys. Oceanogr.*, 14:378–391.
- Cannariato, K.G., Kennett, J.P., and Behl, R.J., 1999. Biotic response to late Quaternary rapid climate switches in Santa Barbara Basin: ecological and evolutionary implications. *Geology*, 27:63–66.
- Hickey, B.M., 1979. The California Current System: hypotheses and facts. *Prog. Oceanogr.*, 8:191–279.
- , 1998. Coastal oceanography of western North America from the tip of Baja California to Vancouver Island. In Robinson, A.R., and Brink, K.H. (Eds.), *The Sea: The Global Coastal Ocean* (Vol. 11): *Regional Studies and Syntheses*: New York (Wiley), 343–397.
- Hollister, C.D., and Heezen, B.C., 1972. Geological effects of ocean bottom currents: western North Atlantic. In Gordon, A.L. (Ed.), *Studies in Physical Oceanography* (Vol. 2): New York (Gordon and Breach), 37–66.
- Hollister, C.D., and McCave, I.N., 1984. Sedimentation under deep-sea storms. *Nature*, 309:220–225.
- Kennett, J.P., 1995. Latest Quaternary benthic oxygen and carbon isotope stratigraphy: Hole 893A, Santa Barbara Basin, California. In Kennett, J.P., Baldauf, J.G., and Lyle, M. (Eds.), *Proc. ODP, Sci. Results*, 146 (Pt. 2): College Station, TX (Ocean Drilling Program), 3–18.
- Kennett, J.P., Baldauf, J.G., and Lyle, M. (Eds.), 1995. *Proc. ODP, Sci. Results*, 146 (Pt. 2): College Station, TX (Ocean Drilling Program).
- Kennett, J.P., and Ingram, B.L., 1995. A 20,000-year record of ocean circulation and climate change from the Santa Barbara Basin. *Nature*, 377:510–512.
- Lyle, M., Koizumi, I., Richter, C., et al., 1997. *Proc. ODP, Init. Repts.*, 167: College Station, TX (Ocean Drilling Program).
- Martinson, D.G., Pisias, N.G., Hays, J.D., Imbrie, J., Moore, T.C., Jr., and Shackleton, N.J., 1987. Age dating and the orbital theory of the ice ages: development of a high-resolution 0 to 300,000-year chronostratigraphy. *Quat. Res.*, 27:1–29.
- McCave, I.N., 1985. Sedimentology and stratigraphy of box cores from the HEBBLE site on the Nova Scotian continental rise. *Mar. Geol.*, 66:59–89.
- McCave, I.N., Manighetti, B., and Robinson, S.G., 1995. Sortable silt and fine sediment size/composition slicing: parameters for palaeocurrent speed and palaeoceanography. *Paleoceanography*, 10:593–610.
- McCave, I.N., and Syvitski, J.P.M., 1991. Principles and methods of geological particle size analysis. In Syvitski, J.P.M. (Ed.), *Principles, Methods, and Application of Particle Size Analysis*: Cambridge (Cambridge Univ. Press), 3–21.
- Morris, R.M., and Behl, R.J., 1998. X-Ray computed tomography reveals correlation between bioturbated continental slope sediments and global climatic fluctuation. *AAPG Annu. Meet.*, CD-ROM.
- Mulder, T., and Syvitski, J.P.M., 1995. Turbidity currents generated at river mouths during exceptional discharge to the world oceans. *J. Geol.*, 103:285–299.
- Neumann, A.C., and Hearty, P.J., 1996. Rapid sea-level changes at the close of the last interglacial (substage 5e) recorded in Bahamian island geology. *Geology*, 24:775–778.
- Normark, W.R., Piper, D.J.W., and Hiscott, R.N., 1998. Sea level controls on the textural characteristics and depositional architecture of the Hueneme and associated submarine fan systems, Santa Monica Basin, California. *Sedimentology*, 45:53–70.
- Ramp, S.R., Rosenfeld, L.K., Tisch, T.D., and Hicks, M.R., 1997. Moored observations of the current and temperature structure over the continental slope off central California, I. A basic description of the variability. *J. Geophys. Res.*, 102:22877–22902.
- Singer, J.K., Anderson, J.B., Ledbetter, M.T., McCave, I.N., Jones, K.P.N., and Wright, R., 1988. An assessment of analytical techniques for the size analysis of fine-grained sediments. *J. Sediment. Petrol.*, 58:534–543.
- Trask, P.D., 1952. Source of beach sand at Santa Barbara, California as indicated by mineral grain studies. *Univ. Calif. Tech. Rep. Eng.*, Ser. 14.
- Van Wagoner, J.C., Mitchum, R.M., Campion, K.M., and Rahmanian, V.D., 1990. *Siliciclastic Sequence Stratigraphy in Well Logs, Cores, and Outcrops: Concepts for High-Resolution Correlation of Time and Facies*. AAPG Methods Explor. Ser., 7.
- Wilgus, C.K., Hastings, B.S., Kendall, C.G.S.C., Posamentier, H.W., Ross, C.A., and Van Wagoner, J.C. (Eds.), 1988. *Sea-level Changes: an Integrated Approach*. Spec. Publ.—Soc. Econ. Paleontol. Mineral., 42.

Date of initial receipt: 2 November 1998

Date of acceptance: 5 August 1999

Ms 167SR-201